Microsegregation effects on the thermal conductivity of silicon-germanium alloys

Yongjin Lee and Gyeong S. Hwang

Citation: J. Appl. Phys. **114**, 174910 (2013); doi: 10.1063/1.4828884
View online: http://dx.doi.org/10.1063/1.4828884
View Table of Contents: http://jap.aip.org/resource/1/JAPIAU/v114/i17
Published by the AIP Publishing LLC.

Microsegregation effects on the thermal conductivity of silicon-germanium alloys

Yongjin Lee and Gyeong S. Hwang[a)]
Department of Chemical Engineering, University of Texas, Austin, Texas 78712, USA

(Received 26 July 2013; accepted 21 October 2013; published online 6 November 2013)

A silicon-germanium (SiGe) alloy is a promising candidate for thermoelectric materials; while it shows a significantly reduced thermal conductivity (κ) as compared to pure Si and Ge, the κ values obtained from previous experiments and computations tend to be widely scattered. We present here a computational analysis of thermal transport in SiGe, particularly the effects of the local segregation (microsegregation) of alloying elements. Our nonequilibrium molecular dynamics simulations confirm the strong dependence of κ on the Si:Ge ratio and the occurrence of the minimum κ around $Si_{0.8}Ge_{0.2}$, consistent with existing experimental observations. Moreover, our study clearly demonstrates that the κ of $Si_{0.8}Ge_{0.2}$ increases substantially and monotonically as Ge atoms undergo segregation; that is, the magnitude of alloy scattering is found to be sensitive to homogeneity in the distribution of alloying elements. Nonequilibrium Green's function analysis also shows that such microsegregation enhances phonon transmission due to the reduced number of scattering centers. The findings highlight that distribution homogeneity, along with composition, can be a critical factor in determining the κ of SiGe alloys. © *2013 AIP Publishing LLC*. [http://dx.doi.org/10.1063/1.4828884]

I. INTRODUCTION

Since the 1960s, SiGe alloys have received much attention as one of the promising candidates for thermoelectric (TE) energy conversion. Due to increased need for renewable energy sources in recent years, a significant amount of both experimental and theoretical efforts has been undertaken to find effective ways to enhance the performance of TE materials; the TE efficiency is conventionally measured by the dimensionless figure of merit $ZT = S^2\sigma T/\kappa$,[1,2] where S the Seebeck coefficient, σ is the electrical conductivity, κ is the thermal conductivity, and T is the absolute temperature.

It is now well accepted that the scattering of phonons due to the mass difference between Si and Ge is primarily responsible for the relatively high ZT of SiGe by suppressing κ, as compared to pure Si and Ge.[3,4] According to earlier experiments,[5–8] the κ of undoped (or lightly doped) $Si_{1-x}Ge_x$ would be as low as 5–10 $Wm^{-1}K^{-1}$ at 300 K when $x = 0.2$–0.3, substantially less than 156.38 (60) $Wm^{-1}K^{-1}$ (Refs. 9 and 10) in Si (Ge). In order to further reduce the κ of SiGe beyond the so-called alloy limit, several attempts[11–16] have been made by introducing point-like defects, chemical impurities, and/or grain boundaries. For instance, nanostructured p-type $Si_{0.8}Ge_{0.2}$ (Refs. 14–16; produced by high-pressure sintering of nanopowders) exhibits very low κ ($\approx$ 2–3 $Wm^{-1}K^{-1}$), resulting in a high ZT value approaching to 1 at 900–950 °C; the substantial reduction of κ has been thought be largely due to increased phonon scattering by nanograins.

In addition, previous experimental work showed that the κ of alloys can be reduced by embedding nanoparticles,[17–19] perhaps due to the interplay between alloy scattering and scattering by embedded nanoparticles. A recent molecular dynamics (MD) study also predicted a drastic reduction in κ when Ge nanoparticles (with diameters of around 1.4–1.6 nm) were embedded in a crystalline Si matrix, as compared to the corresponding random SiGe alloy.[20] Furthermore, a few previous experimental studies[15,21,22] have suggested the possibility that Si and Ge atoms could remain locally segregated in mechanically alloyed SiGe samples; that is, high-energy ball-milling of Si and Ge chunks may not always lead to a random distribution of Si and Ge atoms. While the possible inhomogeneous distribution (microsegregation) would depend on sample preparation conditions, it may affect the degree of alloy scattering and thus thermal transport. Hence, it can be instructive to examine the microsegregation effect on the κ of SiGe alloys.

In this paper, we present a classical MD study of thermal transport in bulk SiGe as a function of composition and microsegregation. First, the κ variation of $Si_{1-x}Ge_x$ with x is evaluated; overall the dependence of κ on x is shown to be consistent with existing experimental data, but the predicted minimum κ is substantially smaller than experimental values. Next, we examine the effect of microsegregation by comparing the κ values of $Si_{0.8}Ge_{0.2}$ with and without Ge microsegregation. The results suggest that the homogeneity in the distribution of alloying elements, along with composition, can be a critical factor in determining the κ of alloys. We also briefly discuss possible impacts of the microsegregation effect on the wide scattering of experimental data and the discrepancy between experimental and MD studies. A nonequilibrium MD (NEMD) method[23] with the Stillinger-Weber (SW) potential model[24] is used to calculate the κ of SiGe alloys, while the SW parameters are modified using the first-principles-based force-matching method.[25]

a)Author to whom correspondence should be addressed. Electronic mail: gshwang@che.utexas.edu

II. COMPUTATIONAL METHODS

In NEMD simulations, using the Müller-Plathe method,[23] a temperature gradient (ΔT) (in the direction of the flow) was obtained from an imposed heat flux (J) to determine the value of κ ($=-J/\Delta T$). As illustrated in Fig. 1, the simulation box (that was subdivided into thin slabs) consists of heat source (indicated as S_H) and heat sink (S_C) layers, two intermediate (I) layers, and two buffer (B) layers; all layers have the same composition (Si:Ge ratio). Periodic boundary conditions were imposed in the x, y, and z directions, while heat conduction was allowed to occur only in the z direction. The cross-section of the rectangular box consists of 10×10 units (corresponding to 400 atoms). The S_H/S_C and B layer thicknesses were set at respective L_S and L_B values corresponding to one (or 400 atoms) and ten (or 4000 atoms) units, respectively, in the axial $\langle 100 \rangle$ direction, while L_I was varied from 40, 80, 120 to 160 units (corresponding to 16 000, 32 000, 64 000, and 128 000 atoms) depending on the total simulation cell length (L_{tot}). Following Vegard's law, the lattice parameter of $Si_{1-x}Ge_x$ (a_{SiGe}) was approximated using linear interpolation between the Si and Ge lattice constants (from density functional theory-generalized gradient approximation (DFT-GGA) calculations), i.e., $a_{SiGe} = (1-x)a_{Si} + xa_{Ge}$, where $a_{Si} = 5.4571$ Å and $a_{Ge} = 5.7564$ Å.

The heat flux was imposed in the z direction by adding (subtracting) nontranslational kinetic energy to a group of atoms in the heat source (sink) layer. After reaching steady state, the temperature profile was obtained. The instantaneous local kinetic temperature in a thin slab is given by $\frac{3}{2}Nk_BT_{MD} = \frac{1}{2}\sum_{i=1}^{N} mv_i^2$, where N is the number of atoms in a system, k_B is the Boltzmann constant, v_i is the velocity of atom i, and m is the atomic mass. If the temperature is below the Debye temperature (T_D), quantum corrections to the calculated temperature (T_{MD}) and thus thermal conductivity (κ_{MD}) are necessary; the correction can be made by $\kappa = \kappa_{MD}\frac{dT_{MD}}{dT}$.[26] The T_D for $Si_{1-x}Ge_x$ is approximated by $T_D(Si_{1-x}Ge_x) = (1-x)T_D(Si) + xT_D(Ge)$,[27] where $T_D(Si) = 645$ K (Ref. 10) and $T_D(Ge) = 374$ K.[10]

The κ of bulk $Si_{1-x}Ge_x$ was obtained by extrapolating finite-size results to infinite size, as described in Ref. 28; all κ values reported hereafter are after quantum corrections, unless stated otherwise. For each of the $Si_{1-x}Ge_x$ systems considered, five independent NEMD simulations were performed with different atomic arrangements and initial velocity distributions. All NEMD simulations were performed using LAMMPS (Large-scale Atomic and Molecular Massively Parallel Simulator)[29] with a time step of 1 fs; a detailed description of the simulation steps can be found in Ref. 30.

For NEMD simulations, we employed a general form of SW potential function which includes two-body (stretching) and three-body (bending) terms. Since the original SW parameter sets[24,31] have a tendency to overestimate the κ of Si,[28] we previously modified the potential parameters using a force-matching method[25] based on DFT calculations. Using the same approach, we also reoptimized the SW parameters for Si-Ge and Ge-Ge interactions.

In this regard, the DFT force data were obtained by displacing one selected atom in the x, y, and z directions by 0.2 Å; the magnitude of the displacement was determined from test calculations with different values greater than the mean atomic displacement of about 0.147 Å (Ref. 32) [0.077 Å (Ref. 33)] in Ge (Si) at room temperature. The restoring forces acting on the displaced atom and its 4 first- and 12 second-nearest neighbors were considered to be matched in the SW parameter adjustments. We used a 64-atom cubic supercell consisting of 1 Ge and 63 Si atoms for the Si-Ge force data, while 64 Si (Ge) atoms for the Si-Si (Ge-Ge) force data. All DFT calculations were performed within the Perdew-Wang 91 generalized gradient approximation (GGA-PW91 (Ref. 34)), as implemented in the Vienna *Ab initio* Simulation Package (VASP).[35] We used Vanderbilt-type ultrasoft pseudopotentials[36] to represent the interaction between core and valence electrons, and a plane-wave basis set with a kinetic energy cutoff of 160 eV. A $(2 \times 2 \times 2)$ Monkhorst-Pack grid of k points was used for the Brillouin zone sampling.

Table I summarizes the modified SW parameters obtained from the force matching approach based on DFT-GGA [SW(GGA)]. Figure 2 shows the comparisons of the restoring forces from the SW(GGA) and DFT calculations for different $Si_{1-x}Ge_x$ samples ($x = 0.25$, 0.5, and 0.75); note that the SW(GGA) and DFT results are in excellent agreement, while the original parameter sets [SW(ORG)] yield consistently overestimated forces.

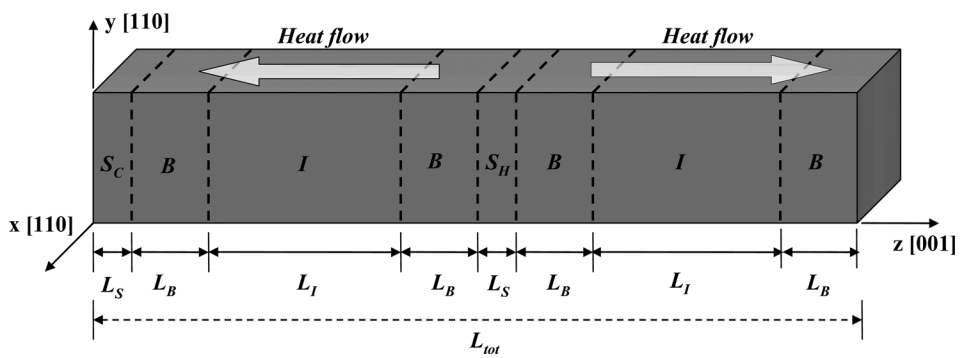

FIG. 1. Schematic illustration of a rectangular simulation domain with periodic boundary conditions imposed in the x, y, and z directions. The simulation cell consists of heat source (S_H), heat sink (S_C), buffer (B), and intermediate (I) layers; temperature gradients used for the thermal conductivity calculation were obtained only from the I layers to avoid any unwanted effects arising from velocity switching-induced nonphysical phonon scatterings in the S_H and S_C regions. Heat flows in two directions due to the periodic boundary condition imposed in the $\langle 100 \rangle$ direction, as indicated.

TABLE I. Stillinger-Weber parameters are modified based on the interatomic forces from first principles calculations for the study of thermal transport in Si, Ge, and SiGe.

	σ	ε (eV)	λ	a	γ	
Si	2.1051937	1.41992	29.5303	1.8	1.2	$A=7.049556277$
Ge	2.221545	1.30665	24.6348	1.8	1.2	$B=0.6022245584$
SiGe	2.141453	1.459299	31.0776	1.843	1.3428	$p=4.0$ $q=0.0$

III. RESULTS AND DISCUSSION

A. Composition effect

With the modified SW parameter, we calculated the κ of bulk $Si_{1-x}Ge_x$ as a function of x; here, Si and Ge atoms were assumed to be *randomly* distributed. As presented in Fig. 3, the κ values of pure Si and Ge are predicted to be $136.65 \pm 9.15\,Wm^{-1}K^{-1}$ and $70.23 \pm 7.32\,Wm^{-1}K^{-1}$ at 300 K, respectively, close to the corresponding experimental values of $156.38\,Wm^{-1}K^{-1}$ (Ref. 9) and $60\,Wm^{-1}K^{-1}$ (Ref. 10); by contrast, the original SW(ORG) parameter sets yield much higher κ values ($243.99 \pm 19.75\,Wm^{-1}K^{-1}$ for Si and $152.25 \pm 17.23\,Wm^{-1}K^{-1}$ for Ge).

For $x<0.2$ or $x>0.8$, the κ of the host (Si or Ge) matrix rapidly drops as the heteroatom (Ge or Si) content (n_i) increases. The reduction of κ with n_i can be well described by an inverse power law relationship, $\kappa \propto n_i^{-\alpha}$; the best fits are given when $\alpha=0.83094$ and 0.99827 for $x<0.2$ and $x>0.8$, respectively. The different values of α clarifies that the introduction of heavy impurities in a light host will cause a greater reduction in κ than the case of light impurities in a heavy host. This is also well supported by the theoretical model suggested by Abeles;[3] that is, the strength of alloy scattering (Γ) due to the mass difference between alloying elements is given by $\Gamma=\sum_i x_i\left(\frac{M_i-M}{M}\right)^2$, where x_i and M_i are the fractional concentration and the atomic weight of element i, respectively, and M is the atomic weight of the alloy ($M=\sum_i x_i M_i$). According to the model, for instance, the scattering strengths are approximated to be 0.024098 in $Si_{0.99}Ge_{0.01}$ ($x_{Si}=0.99$) and 0.003768 in $Si_{0.01}Ge_{0.99}$ ($x_{Si}=0.01$); that is, the scattering strength of Ge in the lighter Si lattice is approximately 6 times greater than that of Si in the heavier Ge lattice although the heteroatom contents are identical at 1 at. %.

For $x=0.2$–0.8, the κ of $Si_{1-x}Ge_x$ shows no significant variation with x. Our simulations predict the minimum κ to be 1–2 $Wm^{-1}K^{-1}$ (corresponding to 0.5–1 mK/W of thermal resistance) around $x=0.2$. The simulated trend of κ with x is overall consistent with existing experimental observations.[5–8] However, the predicted minimum κ is substantially smaller than the experimentally reported values of 5–10 $Wm^{-1}K^{-1}$ at $x\approx0.2$. A couple of likely reasons have been suggested for the discrepancy between the classical MD and experimental results, including possible exaggeration of point defect scattering[37] and insufficient convergence due to relatively small simulation cells.[38] In addition, as mentioned in the introduction, the microsegregation effect may play a certain role in causing the experimental κ values to be larger than the classical MD results; note that previous MD simulations mostly assumed random mixing of Si and Ge atoms. In Sec. III B, we examine the dependence of κ on the local segregation of alloying elements.

B. Microsegregation effect

We examined the variation of κ in $Si_{0.8}Ge_{0.2}$ by changing the extent of Ge segregation. As illustrated in Fig. 4, the segregated $Si_{0.8}Ge_{0.2}$ samples were generated using Monte Carlo (MC) simulations with a relatively reduced Si-Ge bond energy with respect to Si-Si and Ge-Ge bond energies. The extent of segregation can be quantified using the Cowley short range order parameter,[39] defined by $\alpha_i=1-p_i/x_{Si}$, where the subscript i represents the ith neighbor shell from a selected Ge atom, p_i is the probability of having a Si atom in the ith shell, and x_{Si} is the mole fraction of Si. The parameter α_i ranges from 1 to $1-x_{Si}^{-1}$; $\alpha_i>0$ indicates that Ge has a tendency to segregate while $\alpha_i=0$ (i.e., $p_i=x_{Si}$) means a completely random distribution. As summarized in Table II, as Ge atoms undergo segregation, α_1 and α_2 gradually increase while $\alpha_2 \ll \alpha_1$ and $\alpha_3\approx0$. Our calculations predict the κ of $Si_{0.8}Ge_{0.2}$ to monotonically increase with α_1, and $\kappa=2.14\,Wm^{-1}K^{-1}$ at $\alpha_1=0.381$ is about 70% larger than the case of random mixing ($=1.25\,Wm^{-1}K^{-1}$). Although the simple structural model may not explicitly represent the complex potential inhomogeneity of SiGe alloys, the results unequivocally suggest that the local segregation of alloying elements can play an important role in determining κ.

To further investigate the microsegregation effect, we prepared several $Si_{0.8}Ge_{0.2}$ samples by embedding spherical

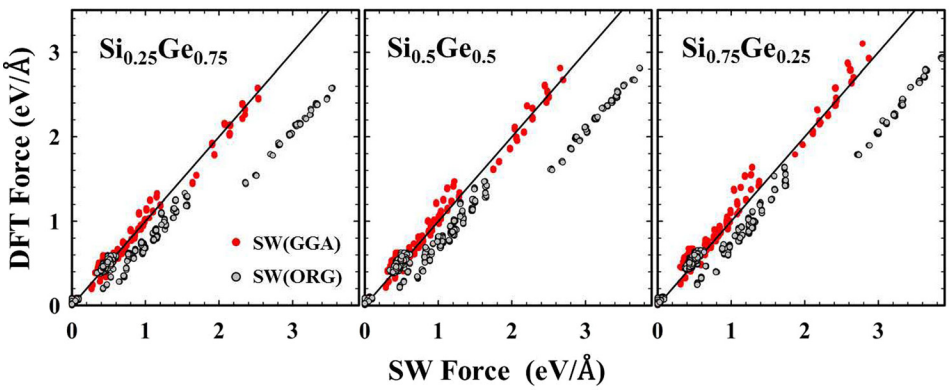

FIG. 2. Parity plots showing discrepancies between DFT and SW predictions for the restoring forces acting on the displaced atom and its first- and second-nearest neighbors in three different SiGe alloys as indicated.

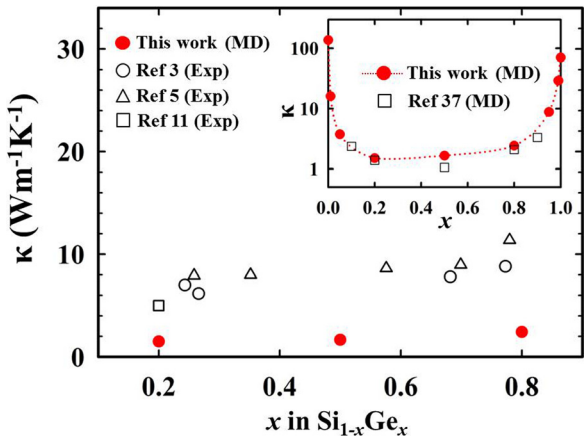

FIG. 3. Predicted variation of the thermal conductivity (κ) of $Si_{1-x}Ge_x$ at 300 K. Solid red (black) circles show the κ values from our NEMD simulations, while open circles, triangles, and squares indicate the experimental values of Abeles,[3] Stohr and Klemm,[5] and Vining,[11] respectively. The inset shows a comparison of κ with previous MD results.[38]

Ge particles of different sizes (ranging from 5 to 293 atoms) in the Si matrix. As illustrated in Fig. 5, embedded Ge particles were randomly positioned but not allowed to overlap each other. Figure 6 shows the variation of κ for the $Si_{0.8}Ge_{0.2}$ samples as a function of Ge particle diameter (D_e); here, D_e is approximated by $(6N_{Ge}V_{Ge}/\pi)^{1/3}$, where N_{Ge} is the number of Ge atoms in the particle and V_{Ge} is the volume per atom for Ge ($=0.0238\,nm^3$ from our DFT-GGA calculation). The κ is predicted to monotonically increase with D_e; note that $\kappa = 4.18\,Wm^{-1}K^{-1}$ at $D_e = 2.37$ nm is about 3.3 times greater than $\kappa = 1.25\,Wm^{-1}K^{-1}$ for the random alloy. The results clearly demonstrate that the κ of SiGe alloys can be sensitive to the local segregation of Si and Ge atoms.

To better understand the role of microsegregation, we examined transmission characteristics of phonons in different $Si_{0.8}Ge_{0.2}$ structures using the nonequilibrium Green's function (NEGF) approach.[40–43] Here, we ignored nonlinear phonon-phonon scatterings, as our primary concern was to understand the dependence of alloy scattering on the local segregation of alloying elements. Considering only elastic scattering events, the ballistic thermal conductance (σ) at a given temperature can be expressed by the Landauer formula;[40,41] $\sigma = \frac{1}{2\pi}\int_0^\infty d\omega\hbar\omega T(\omega)\frac{\partial f}{\partial T}$, where f is the Bose

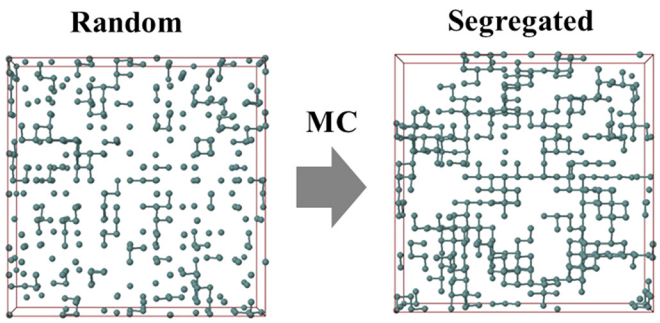

FIG. 4. Schematic cross-sectional views of Ge atoms in $Si_{0.8}Ge_{0.2}$: (left) randomly distributed; (right) segregated. Ge segregation was simulated using a MC method with a relatively reduced Si-Ge bond energy with respect to Si-Si and Ge-Ge bond energies. For clarity, only a part of each $Si_{0.8}Ge_{0.2}$ simulation domain is shown here.

TABLE II. Predicted thermal conductivity (κ) values at 300 K for $Si_{0.8}Ge_{0.2}$ with different degrees of Ge segregation; the segregated $Si_{0.8}Ge_{0.2}$ samples were obtained using Monte Carlo simulations (see Fig. 4). α_i is the Cowley's short range order parameter at the ith neighbor shell.

κ ($Wm^{-1}K^{-1}$)	α_1	α_2	α_3
2.14	0.381	0.079	−0.012
2.11	0.376	0.074	−0.018
2.05	0.360	0.071	−0.019
1.99	0.354	0.060	−0.022
1.85	0.291	0.045	−0.021
1.78	0.272	0.033	−0.017
1.56	0.235	−0.010	−0.014

distribution for phonons. Based on the Caroli formula, the frequency-dependent phonon transmission coefficient is given by $T(\omega) = Tr(G^r\Gamma_L G^a\Gamma_R)$, where G^r (G^a) represents the retarded (advanced) Green's function of the central scattering region and Γ_L (Γ_R) describes the interaction between the left (right) electrode and the central region. Here, the dynamic matrices for the G and Γ calculations were obtained from the second derivative of the SW(GGA) potential energy surface with a displacement of 0.02 Å. Within the NEGF framework, as illustrated in Fig. 7, each calculation system consists of a central scattering alloy region and two semi-infinite Si leads; the axial lengths of the scattering region and each lead were set to 33.13 Å and 5.52 Å, respectively. The $Si_{0.8}Ge_{0.2}$ alloy in the scattering region has randomly distributed Ge atoms or Ge particles (with $D_e = 0.91$, 1.58, or 2.37 nm corresponding to 17, 87, or 293 Ge atoms, respectively).

Figure 8 shows calculated frequency-dependent phonon transmission coefficients for the considered $Si_{0.8}Ge_{0.2}$ systems. With increasing the size of Ge particles (or the degree of microsegregation), the transmission of phonons is found to increase rapidly, except for the low frequency regime

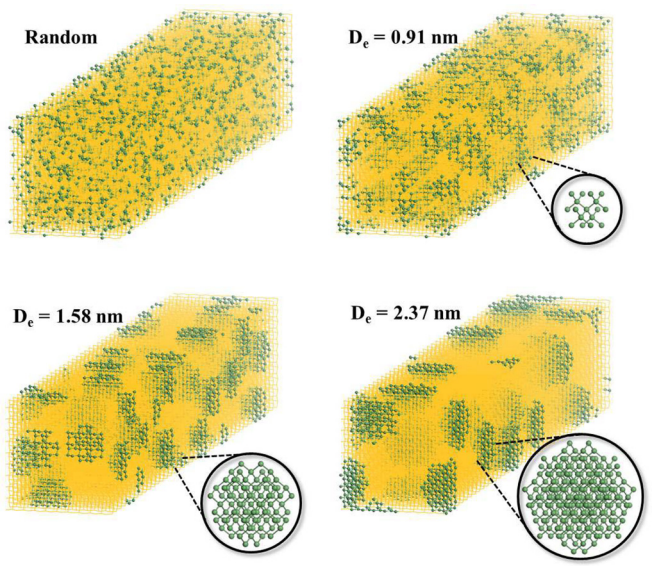

FIG. 5. The various $Si_{0.8}Ge_{0.2}$ configurations show a random distribution of Si and Ge atoms (random) and embedded Ge particles with different diameters ($D_e = 0.91$, 1.58, and 2.37 nm) in the Si matrix. Green (black) balls and yellow lattices represent Ge and Si atoms, respectively.

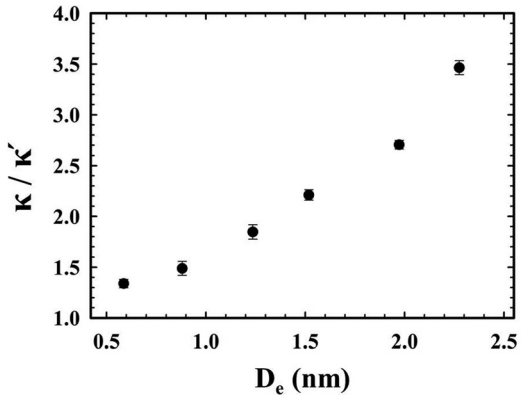

FIG. 6. Predicted variation of the relative thermal conductivity with respect to the random alloy (κ/κ') as a function of the diameter (D_e) of Ge particles embedded in $Si_{0.8}Ge_{0.2}$ (see Fig. 5); note that the predicted κ' for the randomly distributed $Si_{0.8}Ge_{0.2}$ sample is about 1.25 $Wm^{-1}K^{-1}$.

($\omega < 130\,cm^{-1}$). Given that mass disorder is mainly responsible for the reduction of κ in the SiGe alloy, single and paired Ge atoms may act mainly as scattering centers when they are atomically dispersed. On the other hand, when Ge atoms remain locally segregated, scattering by the mass difference would occur at Ge particle-Si matrix interfaces, and also Ge particles may provide additional scattering centers. Therefore, such Ge segregation will reduce the number of scattering centers, thereby increasing phonon transmission, compared to when Ge atoms are homogeneously distributed in the $Si_{0.8}Ge_{0.2}$ matrix. It is also worth noting that the transmission coefficient appears to be rather insensitive to the extent of microsegregation when ω is below 100 cm^{-1}. The transport of such low-frequency (long-wavelength) phonons may undergo scattering mainly due to Ge particles; in this case, phonon transmission can be effectively blocked if the Ge particle concentration is large enough, and thus it becomes no longer a strong function of particle size.[30]

Our study clearly demonstrates that the local segregation (microsegregation) of alloying elements, along with composition, can be a critical factor in determining the κ of alloys; that is, the magnitude of alloy scattering can be sensitive to the homogeneity in distribution of alloying elements. We speculate that the strong microsegregation effect could be

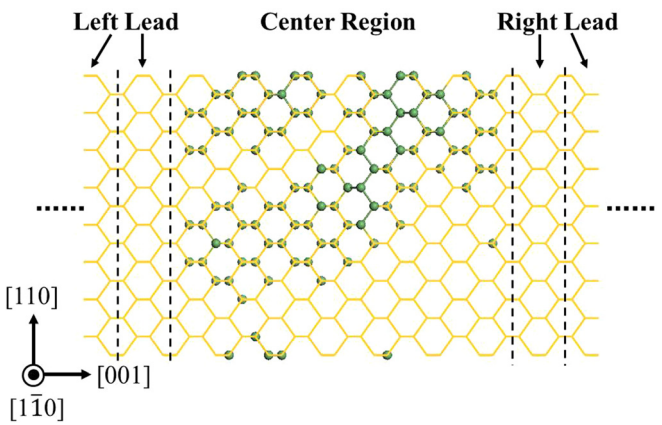

FIG. 7. Schematic diagram showing the domain of our NEGF simulation. Green balls and yellow lines represent Ge atoms and the Si lattice, respectively. The lattice constant of each lead is set at 5.5169 Å.

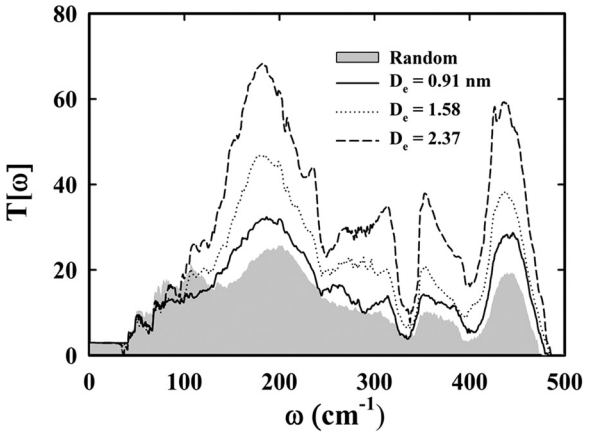

FIG. 8. Frequency-dependent phonon transmission coefficients (T[ω]) calculated for Ge particle-embedded $Si_{0.8}Ge_{0.2}$ with comparison to the random alloy case where Si and Ge atoms are homogeneously distributed.

one of the possible reasons, perhaps along with structural irregularities such as grain boundaries,[13–16] for the wide distribution of the experimentally observed κ values of SiGe; for instance, the κ of $Si_{0.8}Ge_{0.2}$ has been reported to range from 2.5 to 10 $Wm^{-1}K^{-1}$. Note that the experimental samples were mostly obtained via mechanical alloying (ball milling) of Si and Ge chunks. Given that, Si and Ge may not always be fully mixed at the atomic scale, and moreover the local segregation, if any, would strongly depend on sample preparation conditions; if so, this could cause a significant variation in κ from sample to sample. Furthermore, the increase of κ with microsegregation may suggest that the minimum κ would be achieved when Si and Ge atoms are randomly distributed; that is, κ suppression due to alloy scattering could be maximized in the random SiGe alloy. This can be another possible reason why the experimental values of κ are consistently larger than those from classical MD simulations (that assume a random distribution of Si and Ge atoms).

IV. SUMMARY

We examined thermal transport in SiGe using NEMD simulations, with particular focus on the effects of composition and microsegregation. The SW potential parameters employed were optimized by fitting to the restoring forces due to atomic displacements from DFT calculations. The predicted κ values for pure Si and Ge with the modified SW parameters are $136.65 \pm 9.15\,Wm^{-1}K^{-1}$ and $70.23 \pm 7.32\,Wm^{-1}K^{-1}$ at 300 K, respectively, close to experimental data. First, we calculated the κ of bulk $Si_{1-x}Ge_x$ as a function of x; here, Si and Ge atoms were assumed to be randomly distributed. The simulation results are overall consistent with existing experimental observations in that (i) for $x < 0.2$ (or $x > 0.8$), the κ rapidly drops as the Ge (or Si) content increases, (ii) for $x = 0.2$–0.8, the κ shows insignificant variation with x, and (iii) the minimum value of κ occurs around $x = 0.2$. However, the predicted minimum κ of 1–2 $Wm^{-1}K^{-1}$ is substantially smaller than the experimental values of 5–10 $Wm^{-1}K^{-1}$. Next, we calculated the variation of κ in $Si_{0.8}Ge_{0.2}$ by changing the extent of Ge segregation. Here, the segregated samples were generated by

(i) using MC simulations with a relatively reduced Si-Ge bond energy with respect to Si-Si and Ge-Ge bond energies or (ii) embedding spherical Ge particles of different sizes in the Si matrix. Our results clearly show that the κ of $Si_{0.8}Ge_{0.2}$ substantially and monotonically increases as Ge atoms undergo segregation. For instance, the κ of $Si_{0.8}Ge_{0.2}$ with Ge particles of diameter $D_e = 2.37$ nm is predicted to be $4.18\,Wm^{-1}K^{-1}$, about 3.3 times greater than $1.25\,Wm^{-1}K^{-1}$ for the case of random alloy where Si and Ge atoms are homogeneously distributed. Our NEGF analysis also shows significant enhancement of phonon transmission in $Si_{0.8}Ge_{0.2}$ with Ge segregation as compared to the random alloy, which turns out to due to the reduced number of scattering centers. The simple structural models may not explicitly represent the complex potential inhomogeneity in distribution of Si and Ge atoms; nonetheless, our study clearly highlights that the local segregation (microsegregation) of alloying elements, along with composition, can be a critical factor in determining the κ of alloys. We also speculate that the strong microsegregation effect could be one of the possible reasons for the wide distribution of experimental κ values and the large discrepancies with classical MD simulations (which assume a random distribution of Si and Ge atoms). The fundamental understanding would provide some hints on how to modify the SiGe alloy to enhance its thermoelectric properties.

ACKNOWLEDGMENTS

We acknowledge the Robert A. Welch Foundation (F-1535) for their financial support. We would also like to thank the Texas Advanced Computing Center for use of their computing resources.

[1]G. S. Nolas, J. Sharp, and H. Goldsmid, *Thermoelectrics: Basic Principles and New Materials Developments* (Springer, New York, 2001).
[2]*Thermoelectrics Handbook: Macro to Nano*, edited by D. Rowe (CRC Press, Boca Raton, 2006).
[3]B. Abeles, Phys. Rev. **131**, 1906 (1963).
[4]J. Garg, N. Bonini, B. Kozinsky, and N. Marzari, Phys. Rev. Lett. **106**, 045901 (2011).
[5]H. Stohr and W. Klemm, Z. Anorg. Allg. Chem. **241**, 305 (1939).
[6]B. Abeles, D. S. Beers, G. D. Cody, and J. P. Dismukes, Phys. Rev. **125**, 44 (1962).
[7]J. P. Dismukes, L. Ekstrom, E. F. Steigmeier, I. Kudman, and D. S. Beers, J. Appl. Phys. **35**, 2899 (1964).
[8]M. C. Steele and F. D. Rosi, J. Appl. Phys. **29**, 1517 (1958).
[9]R. K. Kremer, K. Graf, M. Cardona, G. G. Devyatykh, A. V. Gusev, A. M. Gibin, A. V. Inyushkin, A. N. Taldenkov, and H. J. Pohl, Solid State Commun. **131**, 499 (2004).
[10]C. Kittel, *Introduction to Solid State Physics*, 7th Ed. (Wiley, New York, 2006).
[11]C. B. Vining, W. Laskow, R. R. Van der Beck, and P. D. Gorsuch, J. Appl. Phys. **69**, 4333 (1991).
[12]D. M. Rowe, V. S. Shukla, and N. Savvides, Nature **290**, 765 (1981).
[13]D. M. Rowe, L. W. Fu, and S. G. K. Williams, J. Appl. Phys. **73**, 4683 (1993).
[14]G. Joshi, H. Lee, Y. Lan, X. Wang, G. Zhu, D. Wang, R. W. Gould, D. C. Cuff, M. Y. Tang, M. S. Dresselhaus, G. Chen, and Z. Ren, Nano Lett. **8**, 4670 (2008).
[15]X. W. Wang, H. Lee, Y. C. Lan, G. H. Zhu, G. Joshi, D. Z. Wang, J. Yang, A. J. Muto, M. Y. Tang, J. Klatsky, S. Song, M. S. Dresselhaus, G. Chen, and Z. F. Ren, Appl. Phys. Lett. **93**, 193121 (2008).
[16]Y. Lan, A. J. Minnich, G. Chen, and Z. Ren, Adv. Funct. Mater. **20**, 357 (2010).
[17]W. Kim, J. Zide, A. Gossard, D. Klenov, S. Stemmer, A. Shakouri, and A. Majumdar, Phys. Rev. Lett. **96**, 045901 (2006).
[18]Y. Bao, W. L. Liu, M. Shamsa, K. Alim, A. A. Balandin, and J. L. Liu, J. Electrochem. Soc. **152**, G432 (2005).
[19]G. Pernot, M. Stoffel, I. Savic, F. Pezzoli, P. Chen, G. Savelli, A. Jacquot, J. Schumann, U. Denker, I. Mőnch, Ch. Deneke, O. G. Schmidt, J. M. Rampnoux, S. Wang, M. Plissonnier, A. Rastelli, S. Dilhaire, and N. Mingo, Nature Mater. **9**, 491 (2010).
[20]J. B. Haskins, A. Kinaci, and T. Çağin, Nanotechnology **22**, 155701 (2011).
[21]J. S. Lannin, Solid State Commun. **19**, 35 (1976).
[22]K. Owusu-Sekyere, W. A. Jesser, and F. D. Rosi, Mater. Sci. Eng., B **3**, 231 (1989).
[23]F. Muller-Plathe, J. Chem. Phys. **106**, 6082 (1997).
[24]F. H. Stillinger and T. A. Weber, Phys. Rev. B **31**, 5262 (1985).
[25]Y. Lee and G. S. Hwang, Phys. Rev. B **85**, 125204 (2012).
[26]J. E. Turney, A. J. H. McGaughey, and C. H. Amon, Phys. Rev. B **79**, 224305 (2009).
[27]F. Schaffler, *Properties of Advanced Semiconductor Materials: GaN, AlN, InN, BN, SiC, SiGe* (Wiley, New York, 2001).
[28]P. K. Schelling, S. R. Phillpot, and P. Keblinski, Phys. Rev. B **65**, 144306 (2002).
[29]S. Plimpton, J. Comput. Phys. **117**, 1 (1995).
[30]Y. Lee, S. Lee, and G. S. Hwang, Phys. Rev. B **83**, 125202 (2011).
[31]K. Ding and H. C. Andersen, Phys. Rev. B **34**, 6987 (1986).
[32]*Group IV Elements, IV-IV and III-V Compounds. Part A—Lattice Properties, Landolt-Börnstein—Group III Condensed Matter Volume 41A1a*, edited by O. Madelung, U. Rossler, and M. Schulz (Springer, 2001).
[33]C. Flensburg and R. F. Stewart, Phys. Rev. B **60**, 284 (1999).
[34]J. P. Perdew and Y. Wang, Phys. Rev. B **45**, 13244 (1992).
[35]G. Kresse and J. Furthmuller, *VASP The Guide* (Vienna University of Technology, Vienna, 2001).
[36]D. Vanderbilt, Phys. Rev. B **41**, 7892 (1990).
[37]A. Skye and P. K. Schelling, J. Appl. Phys. **103**, 113524 (2008).
[38]Y. He, I. Savić, D. Donadio, and G. Galli, Phys. Chem. Chem. Phys. **14**, 16209 (2012).
[39]J. M. Cowley, Phys. Rev. **77**, 669 (1950).
[40]J.-S. Wang, J. Wang, and J. T. Lű, Eur. Phys. J. B **62**, 381 (2008).
[41]J.-S. Wang, J. Wang, and N. Zeng, Phys. Rev. B **74**, 033408 (2006).
[42]N. Mingo and L. Yang, Phys. Rev. B **68**, 245406 (2003).
[43]W. Zhang, N. Mingo, and T. S. Fisher, J. Heat Transfer **129**, 483 (2007).